

Study on transport pathway in oxide nanowire growth by using spacing-controlled regular array

Annop Klamchuen,¹ Takeshi Yanagida,^{1,2,a)} Masaki Kanai,¹ Kazuki Nagashima,¹ Keisuke Oka,¹ Sakon Rahong,¹ Meng Gang,¹ Mati Horprathum,^{1,3} Masaru Suzuki,⁴ Yoshiki Hidaka,⁴ Shoichi Kai,⁴ and Tomoji Kawai^{1,b)}

¹Institute of Scientific and Industrial Research, Osaka University, 8-1 Mihogaoka, Ibaraki, Osaka 567-0047, Japan

²PRESTO, Japan Science and Technology Agency, 4-1-8 Honcho, Kawaguchi, Saitama 332-0012, Japan

³Photonic Technology Laboratory, National Electronics and Computer Technology Center, Pathumthani 12120, Thailand

⁴Department of Applied Quantum Physics and Nuclear Engineering, Faculty of Engineering, Kyushu University, 744 Motoooka, Nishi-ku, Fukuoka 819-0395, Japan

(Received 5 September 2011; accepted 19 October 2011; published online 8 November 2011)

Metal oxide nanowires formed via vapor-liquid-solid (VLS) process are promising nanoscale building blocks. Although understanding material transport pathways across three phases is crucial to realize well-defined oxide nanowires, such knowledge is unfortunately far from comprehensive. Here we investigate the material transport pathway in VLS grown MgO nanowires by utilizing spacing-controlled regular array. Defining the regular spacing of catalysts allows us to extract the information of transport pathway for each catalyst. We found the significant contribution of vapor phase transport pathway rather than the surface diffusion transport. This result highlights the critical role of re-evaporation process on VLS oxide nanowires. © 2011 American Institute of Physics. [doi:10.1063/1.3660246]

Metal oxide nanowires are promising building blocks for nanodevice applications due to their fascinating physical properties such as transparent conductivity, ferromagnetism, ferroelectricity, power-generation, and nonvolatile memory effect, which are hardly attainable with conventional semiconductor materials.¹⁻⁴ In particular, vapor-liquid-solid (VLS) grown oxide nanowires have attracted much attention due to the controllability of the size and the spatial location. However, the intrinsic complexity of material transport pathway across three phases in VLS process has held back the precise control and formation of well-defined oxide nanowires.⁵⁻⁷ In fact, such controllability is strongly required to realize highly integrated nanodevices using nanowires. Most previous works as to VLS grown oxide nanowires have utilized the metal catalysts on the substrate surface to grow oxide nanowires.⁸⁻¹¹ One of reasons why it had been difficult to extract the material transport pathway during VLS is the use of random distribution of metal catalysts on the substrate surface.⁸⁻¹¹ Recently, Borgstrom *et al.* have investigated material transport pathways of VLS grown GaP nanowires by introducing a spacing-controlled regular array.¹² Use of the spacing-controlled regular array allows us to extract the material transport pathways for each catalyst, which is clearly difficult to obtain for random array systems. In this study, we investigate the material transport pathway in VLS grown MgO nanowires by utilizing such spacing-controlled regular array. We found the significant contribution of vapor phase transport pathway on VLS grown oxide nanowires, which differs from some previous implications based on the presence of long surface diffusion phenomena.^{13,14}

Regular arrays of MgO nanowires were fabricated by the Au dot catalysts positioned in a hexagonal pattern on

MgO (100) single crystal substrates. The Au catalyst patterns on non-conductive substrates were fabricated by electron beam lithography (EBL). The spacing between Au dot catalysts was varied from 150 to 5000 nm. The diameter and the thickness of Au catalyst were 50 and 7 nm, respectively.¹⁵ The growth rate data of non-patterning is defined as a data when the nanowires are grown when using the random distribution of Au catalyst on the substrate surface.¹⁶⁻¹⁸ The nanowire density of non-pattern was 4.3×10^8 nanowires/mm², which is higher even compared with that for spacing-controlled nanowires of 150 nm spacing (5.1×10^7 nanowires/mm²).

Figure 1 shows the typical images of patterned Au catalysts and fabricated MgO nanowires. Utilizing the spacing-controlled regular array, we examine the material transport pathway during VLS process. Two major material transport pathways in VLS process have been suggested for the incorporation of supplied species into catalysts.^{13,14,19} One is the direct impinging pathway and the other is the surface migration pathway.^{13,14,19} The direct impinging contribution must be dominated by the amount of the species which directly arrive at the catalyst surface. The amount can be estimated from the film thickness prepared at room temperature, because the re-evaporation of Mg species becomes negligible at such low temperature.²⁰ Figure 2 shows the growth rate of MgO nanowires (length/time) when varying the wire spacing, and the data of film growth rate is also shown for the comparison. The nanowire growth rate was found to be much larger than that of film, indicating the minor contribution of direct impinging pathway. In other words, the catalyst must collect the species from surroundings via the migration pathway. Above 200 nm spacing, the nanowire growth rate was almost independent of the wire spacing, whereas below 200 nm the growth rate decreased with decreasing the

^{a)}Electronic mail: yanagi32@sanken.osaka-u.ac.jp.

^{b)}Electronic mail: kawai@sanken.osaka-u.ac.jp.

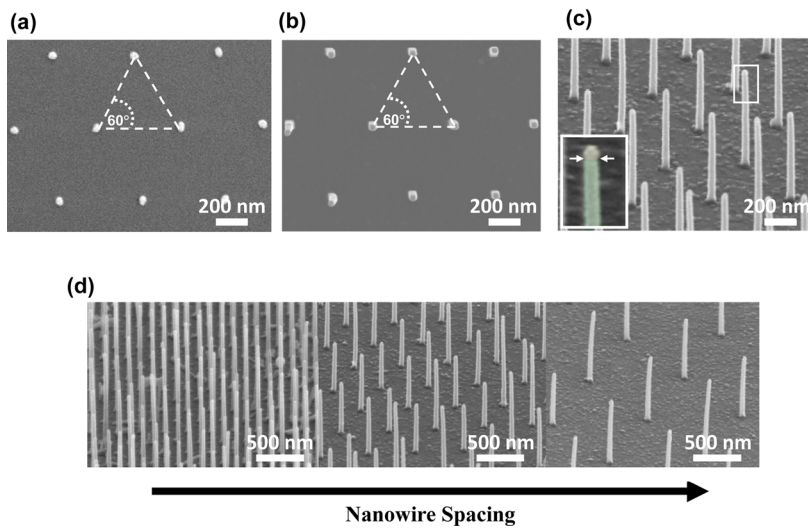


FIG. 1. (Color online) (a) Au dot pattern as catalyst before nanowire growth, (b) the top view, (c) the tilted (60°) images of MgO nanowire arrays grown on MgO (100) substrates and (d) the FESEM images of the nanowire arrays with the interwire spacing of 150, 500, and 1000 nm, respectively. Inset in (c) shows the Au catalyst at the tip of MgO nanowires.

spacing. These two regimes can be defined as “independent regime” and “material competition regime,” respectively.^{13,14} Here we question which type of migration pathways causes the two regimes, although most previous investigations have considered the surface migration as the major migration pathway.^{13,14,19} We discuss by using the term “collection area,” which corresponds to the tentative area around each catalyst by assuming that all species arriving at the “collection area” can be absorbed by the single catalyst dot. Thus, the radius of this area gives an indication of migration length of the supplied species. Since the total material volume must be conserved, the collection area can be derived from the nanowire growth rate in the independent regime and the flux from the source (film growth rate). From the data in Fig. 2, the collection area was estimated to be a circle area with the radius of about 100 nm. Although this estimated value is consistent with the half value of the spacing at the boundary between the independent regime and the material competition regime in Fig. 2, we will discuss this matter as the incorporation efficiency in later section. It has been considered that the collection area is closely related to the surface diffusion length of the species.^{13,14} Since the diffusion is a phenomenon based on independent random-walk motion of each element, not straight forward motion, this means that the length of the migration trajectory must be much longer than the collective area radius of 100 nm. In our MgO nanowires, oxygen could be incorporated from surroundings at 10^{-3} Pa of oxygen partial pressure, and Mg must be supplied only from the target. Therefore it is reasonable to assume that Mg migration is responsible for the migration events. Another possibility is MgO dimer migration, but the probability to form such dimer must be rather low due to the low oxygen partial pressure employed. Moreover, the heavier dimers generally have shorter migration length than lighter single atom. For these reasons, we consider the Mg migration on the MgO substrate surface. Recently, Geneste *et al.* has calculated the adsorption and diffusion of Mg on MgO (001) surface by using a first principle calculation.²¹ Based on their calculated values, we can estimate the diffusion length of Mg on MgO (100) surface, λ_{Mg} , by following formula: $\lambda_{Mg}^2 = a^2 \exp(- (E_{ad} - E_d)/k_B T)$, where a is the distance between the

two neighboring equilibrium position for the diffusing particle, E_{ad} is adsorption energy, E_d is diffusion barrier, k_B is Boltzmann constant, and T is temperature.²¹ For our experimental configurations with the growth temperature of 800°C , the estimated value of the λ_{Mg} is about 1 nm. This value is two orders of magnitude smaller than our experimental data (100 nm). Thus, this discrepancy indicates that the surface diffusion alone cannot explain the major material transport pathway. Therefore we consider the other possible transport pathway of adatom incorporation process. Since above results highlighted the re-evaporation events of Mg species, it is reasonable to speculate that the main process of Mg incorporation into the catalysts comes from re-evaporated Mg transport in the vapor phase. This scenario is consistent with our previous report on SnO_2 nanowire growth.⁵ The inset of Fig. 3 shows the growth rate of MgO thin films deposited under 800°C as a function of oxygen partial pressure. Below the oxygen partial pressure of 10^{-2} Pa, the growth rate of MgO thin films was almost zero, indicating the absence of VS thin films growth. Our results consistently suggest that the enhancement of re-evaporation is an essential mechanism to realize VLS nanowire growth. This vapor phase transport, which has not been considered in previous works, should be added as the third material transport pathway in addition to the direct impinging and surface diffusion pathways.

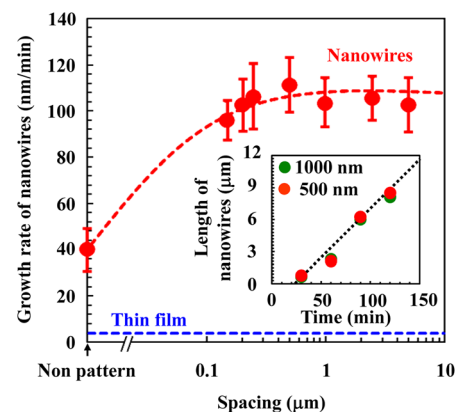


FIG. 2. (Color online) Growth rate of MgO nanowire as a function of the interwire-spacing. The dotted line is the growth rate of the thin film prepared at room temperature. Inset shows the nanowire length as a function of the growth time with interwire distance of 1000 nm.

Finally, we discuss one unique behavior, which is the incorporation efficiency of supplied species into the catalyst. The efficiency is defined as the ratio of the nanowire total volume per unit area to supplied flux. Figure 3 shows the nanowire total volume per unit area when varying the wire spacing. The supplied flux was determined by the film growth rate. Around the spacing near 200 nm, the total volume of nanowire is nearly equal to the film volume. This is also consistent with the boundary between the independent regime and the material competition regime. This means that the most of all supplied species contributed to the nanowire formation when the catalyst spacing is enough short. As mentioned above, the nanowire growth should be enhanced by the re-evaporation which generally increases the escaping probability of adatom from the substrate surface. Thus such high incorporation efficiency is not easily understood. Although we cannot give a conclusive explanation for this behavior in this stage, we suggest that the nanowire structure itself can give large effects on the high efficiency. Under the pressure of 1 Pa for the wire growth, the mean free path of atoms in the vapor phase must be order of millimeter, and this is much longer than the interwire spacing or nanowire length. Therefore, the motion of the re-evaporated atom would be translational rather than diffusion, and the flight length must be very long. If the momentum direction of the re-evaporated atom is near perpendicular to the substrate surface, the atom can easily escape from the substrate surface to outer system. If the direction is near parallel to the surface, the atom can re-attach nanowire sidewalls. The attached adatom on the sidewall re-evaporates again after short-period surface migration, and repeats attaching and re-evaporation until the atoms can be absorbed by catalysts or go out to outer system. The escaping probability of the atoms from the substrate depends on the solid angle indicating the open space among the nanowire forest, and the solid angle is mainly determined by the ratio between the nanowire length and the interwire spacing. Thus, the escaping probability decreases with elongation of the wire, because the long sidewall of wires can work as effective trap-sites to increase the chance of atom incorporation into the catalyst resulting in wire growth. If our speculation is appropriate, the wire

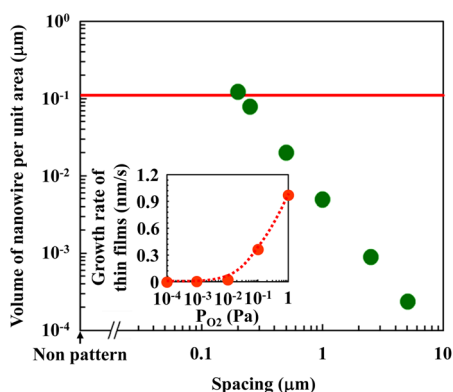


FIG. 3. (Color online) (a) Growth rate of MgO thin films deposited under 800 °C as a function of P_{O_2} and (b) the interwire-spacing dependence of total volume (volume per unit area) for MgO nanowires. The nanowire volumes were estimated from the density, length, and diameter of nanowires. Red line shows the volume of the films prepared at room temperature, i.e., total amount of supplied species.

growth rate must depend on the wire length. Especially the dependency should be large when the wire length is less than the interwire spacing and shorter wire length should be accompanied by lower growth rate. The time series data of the growth rate as shown in the inset of Fig. 2 agrees with such scenario, however further investigations by using *in situ* TEM are required to perform more accurate length measurements in the initial stage of the growth to clarify the origin of the high incorporation efficiency.

This study was in part supported by a Grant-in-Aid for Scientific Research on Innovative Areas [20111004] from MEXT. M.H. was supported by NEXT program. T.K was supported by FIRST.

¹B. S. Kwak, A. Erbil, B. J. Wilkens, J. D. Budai, M. F. Chisholm, and L. A. Boatner, *Phys. Rev. Lett.* **68**, 3733 (1992).

²T. Kimura, T. Goto, H. Shintani, K. Ishizaka, T. Arima, and Y. Tokura, *Nature* **426**, 55 (2003).

³J. P. Locquet, J. Perret, J. Fompeyrine, E. Mäeçhler, J. W. Seo, and G. Van Tendeloo, *Nature* **394**, 453 (1998).

⁴K. Nagashima, T. Yanagida, K. Oka, M. Kanai, A. Klamchuen, J.-S. Kim, B. H. Park, and T. Kawai, *Nano Lett.* **11**, 2114 (2011); K. Oka, K. T. Yanagida, K. Nagashima, M. Kanai, T. Kawai, J. S. Kim, and B. H. Park, *J. Am. Chem. Soc.* **133**, 12482 (2011); K. Nagashima, T. Yanagida, K. Oka, M. Taniguchi, T. Kawai, J. S. Kim, and B. H. Park, *Nano Lett.* **10**, 1359 (2010); K. Oka, T. Yanagida, K. Nagashima, T. Kawai, J. S. Kim, and B. H. Park, *J. Am. Chem. Soc.* **132**, 6634 (2010); K. Oka, K. T. Yanagida, K. Nagashima, H. Tanaka, and T. Kawai, *J. Am. Chem. Soc.* **131**, 3434 (2009).

⁵A. Klamchuen, T. Yanagida, M. Kanai, K. Nagashima, K. Oka, T. Kawai, M. Suzuki, Y. Hidaka, and S. Kai, *Appl. Phys. Lett.* **97**, 073114 (2010).

⁶S. H. Dalal, D. L. Baptista, K. BKTeo, R. G. Lacerda, D. A. Jefferson, and W. I. Milne, *Nanotechnol.* **17**, 4811 (2006).

⁷K. Nagashima, T. Yanagida, K. Oka, H. Tanaka, and T. Kawai, *Appl. Phys. Lett.* **93**, 153103 (2008).

⁸K. Nagashima, T. Yanagida, H. Tanaka, and T. Kawai, *J. Appl. Phys.* **101**, 24304 (2007).

⁹M. H. Huang, Y. Wu, H. Feick, N. Tran, E. Weber, and P. Yang, *Adv. Mater.* **16**, 1348 (2004).

¹⁰Q. Wan, E. N. Dattoli, and W. Lu, *Small* **4**, 451 (2004).

¹¹Q. Wan, E. N. Dattoli, W. Y. Fung, W. Guo, Yn. Chen, X. Pan, and W. Lu, *Nano Lett.* **6**, 2909 (2006).

¹²M. T. Borgström, G. Immink, B. Ketelaars, R. Algra, and E. P. A. M. Bakkers, *Nature Nanotechnol.* **2**, 541 (2007).

¹³L. E. Jensen, M. T. Björk, S. Jeppesen, A. I. Persson, B. J. Ohlsson, and L. Samuelson, *Nano Lett.* **4**, 1961 (2004).

¹⁴A. I. Persson, L. E. Fröberg, S. Jeppesen, M. T. Björk, and L. Samuelson, *J. Appl. Phys.* **101**, 034313 (2007).

¹⁵T. Mårtensson, M. Borgström, W. Seifert, B. J. Ohlsson, and L. Samuelson, *Nanotechnol.* **14**, 1255 (2003).

¹⁶K. Nagashima, T. Yanagida, H. Tanaka, and T. Kawai, *Appl. Phys. Lett.* **90**, 233103 (2007); A. Marcu, T. Yanagida, K. Nagashima, H. Tanaka, and T. Kawai, *J. Appl. Phys.* **102**, 016102 (2007); T. Yanagida, A. Marcu, H. Matsui, K. Nagashima, K. Oka, K. Yokota, M. Taniguchi, and T. Kawai, *J. Phys. Chem. C* **112**, 18923 (2008); A. Marcu, T. Yanagida, K. Nagashima, K. Oka, H. Tanaka, and T. Kawai, *Appl. Phys. Lett.* **92**, 173119 (2008); K. Nagashima, T. Yanagida, A. Klamchuen, M. Kanai, K. Oka, S. Seki, and T. Kawai, *Appl. Phys. Lett.* **96**, 073110 (2010).

¹⁷T. Yanagida, K. Nagashima, H. Tanaka, and T. Kawai, *Appl. Phys. Lett.* **91**, 061502 (2007).

¹⁸T. Yanagida, K. Nagashima, H. Tanaka, and T. Kawai, *J. Appl. Phys.* **104**, 016101 (2008); M. Suzuki, Y. Hidaka, T. Yanagida, A. Klamchuen, M. Kanai, T. Kawai, and S. Kai, *Phys. Rev. E* **83**, 061606 (2011); M. Suzuki, M. Y. Hidaka, T. Yanagida, M. Kanai, T. Kawai, and S. Kai, *Phys. Rev. E* **82**, 011605 (2010).

¹⁹V. G. Dubrovski, N. V. Sibirev, R. A. Suris, G. É. Cirlin, V. M. Ustinov, M. Tchernysheva, and J. C. Harmand, *Semiconductors* **40**, 1075 (2006).

²⁰A. Klamchuen, T. Yanagida, K. Nagashima, S. Seki, K. Oka, M. Taniguchi, and T. Kawai, *Appl. Phys. Lett.* **95**, 053105 (2009); A. Klamchuen, A. T. Yanagida, K. Nagashima, M. Kanai, K. Oka, S. Seki, T. Kawai, M. Suzuki, Y. Hidaka, and S. Kai, *Appl. Phys. Lett.* **98**, 053107 (2011).

²¹G. Geneste, J. Morillo, and F. Finocchi, *J. Chem. Phys.* **122**, 174707 (2005).